The Journal of Chemical Physics

RESEARCH ARTICLE | NOVEMBER 06 2023

Molecular dynamics study of the mechanical properties of drug loaded model systems: A comparison of a polymersome with a bilayer

Damián A. Grillo ; Juan M. R. Albano ; Rufino E. Valladares T. ; Esteban E. Mocskos ; Julio C. Facelli ; Mónica Pickholz ; Marta B. Ferraro

J. Chem. Phys. 159, 174908 (2023)
https://doi.org/10.1063/5.0165478

AIP Publishing

The Journal of Chemical Physics ARTICLE pubs.aip.org/aip/jcp

Molecular dynamics study of the mechanical properties of drug loaded model systems: A comparison of a polymersome with a bilayer

Cite as: J. Chem. Phys. 159, 174908 (2023); doi: 10.1063/5.0165478
Submitted: 28 June 2023 • Accepted: 16 October 2023 •
Published Online: 6 November 2023

Damián A. Grillo,[1,2] Juan M. R. Albano,[2] Rufino E. Valladares T.,[1] Esteban E. Mocskos,[3,4] Julio C. Facelli,[5] Mónica Pickholz,[1,2,a)] and Marta B. Ferraro[1,2]

AFFILIATIONS

[1] Universidad de Buenos Aires, Facultad de Ciencias Exactas y Naturales, Departamento de Física, Buenos Aires, Argentina
[2] CONICET - Universidad de Buenos Aires, Instituto de Física de Buenos Aires (IFIBA), Buenos Aires, Argentina
[3] Universidad de Buenos Aires, Facultad de Ciencias Exactas y Naturales, Departamento de Computación, Buenos Aires, Argentina
[4] Centro de Simulación Computacional p/Aplic Tecnológicas, CONICET, Godoy Cruz, 2390 Buenos Aires, Argentina
[5] Department of Biomedical Informatics, University of Utah, 421 Wakara Way, Suite 140, Salt Lake City, Utah 84108, USA

[a)] **Author to whom correspondence should be addressed:** monicapickholz2@gmail.com

ABSTRACT

In this work we implement a new methodology to study structural and mechanical properties of systems having spherical and planar symmetries throughout Molecular Dynamics simulations. This methodology is applied here to a drug delivery system based in polymersomes, as an example. The chosen model drug was the local anesthetic prilocaine due to previous parameterization within the used coarse grain scheme. In our approach, mass density profiles (MDPs) are used to obtain key structural parameters of the systems, and pressure profiles are used to estimate the curvature elastic parameters. The calculation of pressure profiles and radial MPDs required the development of specific methods, which were implemented in an in-house built version of the GROMACS 2018 code. The methodology presented in this work is applied to characterize poly(ethylene oxide)-poly(butadiene) polymersomes and bilayers loaded with the model drug prilocaine. Our results show that structural properties of the polymersome membrane could be obtained from bilayer simulations, with significantly lower computational cost compared to whole polymersome simulations, but the bilayer simulations are insufficient to get insights on their mechanical aspects, since the elastic parameters are canceled out for the complete bilayer (as consequence of the symmetry). The simulations of entire polymersomes, although more complex, offer a complementary approach to get insights on the mechanical behavior of the systems.

I. INTRODUCTION

The rational design of nanocarriers for specific drugs is a very active area.[1–4] It is essential to have theoretical tools that help in this direction. In this context, Molecular dynamics simulations (MD) stand as a potent tool to achieve a deeper understanding of these systems, and thus guide the rational design of nanocarriers.[5–7] The amount of effort in that direction can be seen in the growth in the number of articles in recent years that harness the capabilities of MD simulations. These simulations have been used to investigated critical aspects such as stability, release kinetics, and drug transport mechanisms within a diverse range of carriers. Among the studied systems, as examples, include nanodroplets,[8] micelles,[9,10] liposomes,[11] and polymersomes,[12] each offering a unique perspective on drug delivery and nanocarrier behavior. For example, in the case of micelles, Razavi *et al.*[10] validated MD simulations of micelles that show a response when applying electric fields and their relationship to drug administration. They designed a new type of micelle with the ability to respond to external stimuli while maintaining solubility in water. This supramolecular micelle was formed by the aggregation of two homopolymers: polystyrene-beta-cyclodextrin and polyethylene-ferrocene oxide (PE-FE), through

guest-host interactions. The study reveals that an electric field serves as a driving force for the reversible assembly and disassembly of micelles. This responsiveness to electric fields may have important implications for controlled drug release applications. On the other hand, Lin *et al.*[12] conducted research on the structural and mechanical properties of polymersomes formed by rod-coil diblock copolymers (RxCy). They explore the morphological phase diagram of RxCy to study the essential physical properties of RxCy polymers through dissipative particle dynamics (DPD) simulations. In the simulation results they obtained that small polymersomes are only observed for short lengths of spiral blocks. Furthermore, the length of the rod block should not be too long and weak π–π stacking is necessary, since the anisotropic rod packing resists, membrane bending and vesicle formation. The study explores the mechanical properties of RxCy polymers, demonstrating that membrane tension reaches a maximum while stretching and bending moduli exhibit a minimum at intermediate coil block lengths. Here we focus here on the implementation of a new tool that can help to access to structural and mechanical information of systems that have spherical and axisymmetric symmetry through Molecular Dynamics simulations and applied it to study a polymersome based drug delivery system.

Polymersomes are artificial vesicles formed by amphiphilic block copolymers that, in recent times, have increased in importance due to the versatility of their applications.[13–16] These systems can self-assemble into a bilayer structure,[17–21] and have the ability to encapsulate hydrophobic compounds within their aqueous cores and hydrophilic ones within their membranes.[22–25] Their chemical versatility allows fine tuning of their properties, such as membrane thickness, elasticity, permeability, etc.[23,24] These properties make them promising candidates as nanocarriers for drug release.[26–28] The stability of polymersome based systems is important for a desired specific application. For instance, when polymersomes are used as drug delivery vehicles their mechanical properties determine their stability during storage and transport. The mechanical stiffness of the polymersome membrane is crucial to maintain the integrity of the encapsulated drugs and prevent their premature release. The intrinsic characteristics of polymersomes are closely related to the structural and mechanical properties of their membranes and, therefore, with the nature of the chosen copolymers,[23,27–29] For instance insights into the mechanical properties of the bilayer can be obtained by calculating the free energy associated with the deformations, also known as elastic free energy. These deformations can be characterized in terms of the principal curvatures, which correspond to the curvatures in the two directions of the membrane deformation,[30–32] but detailed studies of the advantages and limitations of using membrane bilayers as representative model systems of the corresponding polymersomes are lacking.

The specific goal of this work is the implementation and testing of a tool to calculate the pressure profiles that determine the mechanical behavior of systems considered here at the molecular level, to access the elastic curvature properties of both model systems (polymersomes and bilayers) and follow the mechanical properties with the level of charge, which represents valuable information when designing and characterizing polymersomes. Due to the system size, it is possible to access a small polymersome or a flat bilayer corresponding to it copolymer bilayer[33] using coarse-grained model retaining enough detail to correctly reproduce the cooperative phenomena that occur at the mesoscale.[34–37] Thus, we explored two polymersomes model systems: small vesicles and copolymer bilayers (that emulate large radius vesicles), for which we compared pure systems with the systems loaded with prilocaine (PLC), and determined the information that could be extracted from each model system and how it can be used for the design of nanocarriers. Prilocaine was chosen as a model drug since we had parameters of this drug in the context of the coarse grain model, and it allowed us to explore combinations of hydrophilic and hydrophobic drugs.[38]

II. METHODS

A. Molecular dynamics simulations

We studied copolymer bilayers and small polymersomes with and without PLC, as described in Table I. We modeled our systems using a CG approach based on the MARTINI force field.[36,37] The CG model for PEO-PBD copolymers was taken from our previous work.[39] PLC species were modeled using the parametrization developed by Pickholz and Giupponi.[38] Explicit solvation was included in the simulations using the polarizable water (PW) model[40] PEO_{14}-PBD_{22}.

For the neat polymersome model, we have used the Packmol package[41] to build up a spherical vesicle containing 815 and 2326 PEO_{14}-PBD_{22} chains on the inner and outer leaflets respectively, and about 43 000 and 285 000 PW in the inner core and outer region respectively. PLC-loaded systems were obtained by incorporating different number of PLC molecules into the neat systems (keeping the physiological pH ratio pPLC/nPLC $\simeq$ 1.6, see Table I). Considering the affinity of PLC molecules for specific regions depending on their protonation state,[39] the neutral species were encapsulated into the hydrophobic PBD core and protonated ones were distributed between the PEO-PBD interfaces and water.[39] We started our study from fully hydrated neat PEO-PBD systems. As the model for the neat bilayer, we have taken the one used for our previous study,[39]

TABLE I. Summary of simulated systems used in this work. All systems were built up with the copolymer PEO_{14}-PBD_{22} (the subscripts represent the length corresponding to the hydrophilic and hydrophobic blocks).

Type[a]	Label[b]	N_{nPLC}/N_{pPLC}[c]	CG sites[d]	t_{sim}[e] (μs)	t_{note}[f] (hs)
B	Neat	0/0	$\sim 3.5 \times 10^4$	5.0	~100
	N27-P43	27/43			
	N54-P86	54/86			
P	Neat	0	$\sim 1.11 \times 10^6$	3.5	~750
	N500-P800	500/800			
	N1000-P1600	1000/1600			

[a]B = Bilayer, P = Polymersome.
[b]Label are related with the number of neutral (N) and protonated (P) drugs.
[c]N_{nPLC} and N_{pPLC} are the numbers of molecules of the respective species.
[d]The CG sites are the effective force centers onto which the all-atom structure is mapped.
[e]Simulation time.
[f]Total node hours, estimation based on the reference hardware: Intel Xeon E5-2680 v4 processors (14 cores, 2.4 GHz), 256 GB RAM, Nvidia Tesla P100 GPU boards, using one processor and one GPU board for bilayers, and two processors and two GPU boards for polymersomes.

built of 100 PEO_{14}-PBD_{22} chains per monolayer (subscripts represent the lengths of the corresponding blocks) and 9000 polarizable water (PW) molecules.[40] In order to balance the net charge of the system, one chloride counterion (Cl^-) per pPLC molecule was also inserted into the corresponding water regions.

MD simulations were carried out using the GROMACS 2018 package.[42] All simulations were done using the NPT ensemble (semi-isotropic for bilayers, isotropic for polymersomes), periodic boundary conditions (PBC) in all directions, shifted Lennard-Jones (LJ) potential (cutoff radius of 1.2 nm), shifted Coulombic potential (cutoff radius of 1.2 nm) with a relative dielectric constant ϵ_r = 2.5, and time steps of 20 fs. Temperature was equilibrated at 300 K using the Nosé-Hoover thermostat[43] with a coupling constant of 6.0 ps. Pressure was kept at 1 bar using the Parrinello-Rahman barostat[44] with a coupling constant of 6.0 ps and compressibility of 4.5×10^{-5} bar^{-1}. The geometry of water molecules was held fixed by means of LINCS algorithm.[45] For bilayers, the simulations were extended up to 5 μs; the corresponding equilibrium trajectories were obtained on the last 3 μs. For polymersomes, the systems were run up to 3.5 μs, and the equilibrium trajectories were taken on the last 1.5 μs. Details of the simulated systems used in this work, including number of PLC loaded molecules, number of total CG sites, simulation and computational times are shown in Table I.

B. Structural analysis

1. Mass density profiles

The mass density profiles (MDPs) for bilayers were obtained by dividing the systems in 100 slabs along z direction [see Fig. 1(a)] and calculating the average density on the corresponding slabs:

$$MDP(z_s) = \left\langle \frac{m_s}{Ah} \right\rangle \tag{1}$$

where z-direction is the normal to the plane of the bilayer, z_s is the position of slab s in z-direction, A and h are the area and thickness of each slab respectively, m_s is the net mass on slab s, and the brackets $\langle \cdots \rangle$ denote temporal averaging. All MDPs were centered at the bilayer midplane.

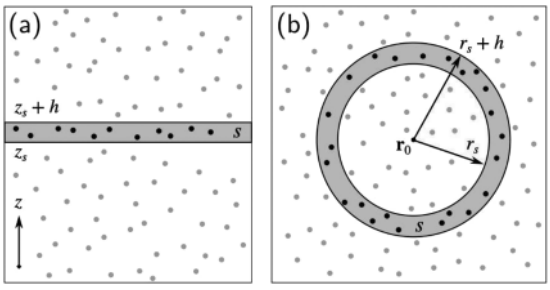

FIG. 1. Schematic illustration of MDPs calculation for (a) planar and (b) spherical systems. For bilayers (a), z-direction was taken as the normal to the plane of the bilayer. For polymersomes (b), $\mathbf{r}_0$ was regarded as the polymersome center.

For polymersomes, radial MDPs were computed using a similar procedure, but dividing the systems in 150 spherical shells centered at $\mathbf{r}_0$ [see Fig. 1(b)] and calculating the average density on the corresponding shells:

$$RMDP(r_s) = \left\langle \frac{m_s}{\left(\frac{4}{3}\right)\pi\left[(r_s + h)^3 - r_s^3\right]} \right\rangle \tag{2}$$

where r_s is the radius of the shell s, h is the thickness of each shell, and m_s is the net mass on shell s.

The centering point $\mathbf{r}_0$ represents the polymersome center; it was determined as the geometric center of the PBD group. For its calculation, we have applied a centering method for periodic systems based on the algorithm proposed by Bai and Breen.[42]

2. Structural properties

Different structural properties of the systems were evaluated by means of the membrane area, the membrane thickness, and the hydrophobic volume per chain (defined as the volume occupied by the hydrophobic core divided by the number of copolymer chains in the system). For bilayers, the membrane area (A) was calculated as $A = b_x b_y$, where b_x and b_y are the box lengths parallel to the plane of the membrane, the membrane thickness (d) as the width at half height of the MDPs of the PBD group, and the hydrophobic volume per chain (V_{hc}) as $V_{hc} = Ad/N_c$, where N_c is the total number of copolymer chains in the system. For polymersomes, we have first defined the inner and outer radii (R_i and R_o respectively) as the two r values for which the MDPs of the PBD group are at half height (R_i the lowest value and R_o the highest one). Using these parameters, we have calculated the inner and outer membrane areas (A_i and A_o respectively) as $A_{i/o} = 4\pi R_{i/o}^2$, the membrane thickness as $d = R_o - R_i$ and the hydrophobic volume per chain as $V_{hc} = (4/3)\pi(R_o^3 - R_i^3)/N_c$. All these quantities were determined by computing their values every 1 ns and obtaining their averages and standard deviations along the equilibrium trajectories.

To compare the changes on the membrane areas for PLC-loaded bilayers and polymersomes at different PLC concentrations, we have defined the normalized membrane area expansion, given by the quantity $\alpha = (A - A_0)/A_0$, where A is the membrane area of the corresponding drug-loaded system and A_0 the membrane area of its associated neat system. In particular, for polymersomes, two α values can be obtained, one for the inner membrane area and the other one for the outer membrane area.

Finally, for PLC-loaded systems we have also quantified the number of adsorbed pPLC molecules per unit area at each PEO-PBD interface. We have denoted these quantities as Γ_i, where i represents the corresponding interface (i = low/upp for the lower/upper interfaces on bilayers, and i = inn/out for the inner/outer interfaces on polymersomes). Calculation details of Γ_i values for the different interfaces are described in the supplementary material.

C. Mechanical analysis

1. Pressure profiles

Pressure profiles are a powerful tool to get insights into the mechanical behavior of the systems at the microscopic level. Depending on the system geometry, different methods have been

developed to compute them. In the next paragraphs, we briefly introduce the calculation of the pressure profiles for planar and spherical systems.

For systems with planar symmetry (bilayers), the local pressure is represented by a diagonal tensor **P** that only depends on the z coordinate.[46,47] It can be written in the form:

$$P(z) = P_{xx}(z)\hat{e}_x\hat{e}_x + P_{yy}(z)\hat{e}_y\hat{e}_y + P_{zz}(z)\hat{e}_z\hat{e}_z \quad (3)$$

where $\hat{e}_x$, $\hat{e}_y$ and $\hat{e}_z$ are the orthogonal unit vectors in cartesian coordinates, and $P_{xx}(z)$, $P_{yy}(z)$, $P_{zz}(z)$ the corresponding components of the pressure tensor.

From the planar symmetry it follows that $P_{xx}(z) = P_{yy}(z)$. Then, tangential and normal components of the pressure tensor are defined as $P_T(z) = [P_{xx}(z) + P_{yy}(z)]/2$ and $P_N(z) = P_{zz}(z)$ respectively. In order to obtain the pressure profiles on bilayers, we have divided the systems in 100 slabs parallel to the plane of the membrane (similarly to the MDPs) and computed $P_T(z)$ and $P_N(z)$ on each slab. Details of the calculation method for $P_T(z)$ and $P_N(z)$ can be found elsewhere.[48–51]

For systems with spherical symmetry (polymersomes), the local pressure tensor is also diagonal and only depends on the r coordinate.[47] It can be written in the form:

$$P(r) = P_{rr}(r)\hat{e}_r\hat{e}_r + P_{\theta\theta}(r)\hat{e}_\theta\hat{e}_\theta + P_{\varphi\varphi}(r)\hat{e}_\varphi\hat{e}_\varphi \quad (4)$$

where $\hat{e}_r$, $\hat{e}_\theta$ and $\hat{e}_\varphi$ are the orthogonal unit vectors in spherical coordinates, and $P_{rr}(r)$, $P_{\theta\theta}(r)$, $P_{\varphi\varphi}(r)$ the corresponding components of the pressure tensor.

Due to the spherical symmetry, we have $P_{\theta\theta}(r) = P_{\varphi\varphi}(r)$. The tangential and normal components of the pressure tensor are defined as $P_T(r) = [P_{\theta\theta}(r) + P_{\varphi\varphi}(r)]/2$ and $P_N(r) = P_{rr}(r)$ respectively. The pressure profiles were calculated by discretizing the systems in 150 spherical shells around the system center (using a similar procedure as for the RMDPs) and computing $P_T(z)$ and $P_N(z)$ on each shell, following the method developed by Nakamura *et al.*[52]

2. Helfrich elastic model

The Helfrich elastic model[30] provides an expression for the elastic free energy per unit area (f) of a fluid membrane in terms of the mean curvature $H = (c_1 + c_2)/2$ and Gaussian curvature $K = c_1c_2$, where c_1 and c_2 are principal curvatures.[53] Within this framework, f can be expressed in the form.[30–32]

$$f(H,K) = 2\kappa(H - H_0)^2 + \bar{\kappa}K \quad (5)$$

where κ is the bending modulus, $\bar{\kappa}$ the Gaussian curvature modulus (also known as saddle-splay modulus), and H_0 the spontaneous curvature.

The elastic parameters κ, $\bar{\kappa}$ and H_0 are defined at zero curvature ($H = K = 0$) and can be estimated for planar bilayers in terms of the integral moments of the $P_T(z) - P_N(z)$ profiles.[53–56] The Helfrich model is an approximate method valid on the low-curvature limit ($H \to 0$, $K \to 0$), thus adequate to describe the elastic behavior of planar bilayers and giant vesicles (1–10 μm diameter).[32]

For small vesicles (15–200 nm diameter), an extension of the Helfrich model developed by Nakamura and Shinoda[32] can be used. This extended model includes the curvature dependency in the elastic parameters without changing the free energy function. Within this formulation, the elastic parameters κ, $\bar{\kappa}$ and H_0 can be defined for any arbitrary curvature. They can be estimated for spherical vesicles through the integral moments of the $P_T(z) - P_N(z)$ profiles.[32]

For all systems studied in this work, we were able to calculate their κ, $\bar{\kappa}$ and H_0 parameters using the corresponding pressure profiles previously obtained from MD simulations. Details of these calculations can be found in the supplementary material. Afterwards, the f values for the corresponding systems were computed from Eq. (5), using $H = K = 0$ for bilayers, and $H = -1/R_s$ and $K = 1/R_s^2$ for polymersomes, where R_s is the radius associated to the surface of tension of the membrane (see details in supplementary material). The minus sign on the H parameter is defined by the convention for the curvature sign taken by Nakamura *et al.* in the extended Helfrich model.[32]

III. IMPLEMENTATION

MDPs for planar systems (bilayers) were computed from MD trajectories using the analysis tools provided in the standard GROMACS 2018 code. Radial MDPs for spherical systems (polymersomes) and pressure profiles for both planar and spherical systems were computed using our own developed tools, implemented as a set of C/C++ modules included in an in-house built version of the GROMACS 2018 code. The pressure profiles calculation is integrated as part of the MD engine and supports serial and parallel processing across multiple cores (using shared memory with OpenMP) and SIMD (Simple Instruction Multiple Data) acceleration for best performance. The code is freely available at https://gitlab.com/damgrillo/gromacs-lpressure. Finally, we have implemented different Python scripts to process the obtained MDPs and pressure profiles to calculate the structural and elastic parameters of the systems as described in the previous sections. The Python scripts are available at https://gitlab.com/damgrillo/plc-python-scripts.

Here, we applied the methodology described below to study and characterization of PEO-PBD bilayers and polymersomes. We first evaluated the neat systems as proof of concept, and we determined the parameters playing a key role on the structural and mechanical aspects of the membrane. Then we applied our approach to study PLC loaded systems, understand their behavior upon loading and the relationship with key structural and elastic parameters.

IV. RESULTS AND DISCUSSION

A. Comparison of neat systems

Figure 2 shows representative snapshots of the equilibrated neat systems. For both cases, we observe the core of the membrane formed by the hydrophobic PBD (pink) surrounded by hydrophilic PEO (purple) and water (cyan).

Insights on the local organization of the components and the local pressure distribution across the systems can be obtained from the MDPs and pressure profiles, illustrated in Fig. 3. As a general remark, we emphasize that the bilayer profiles are essentially symmetric around the bilayer midplane ($z \sim 0$ nm), while the polymersome profiles are inherently asymmetric around the mean radius ($r \sim 11$ nm). The MDPs for the neat bilayer and polymersome are illustrated in Figs. 3(a)–3(c) respectively. These profiles

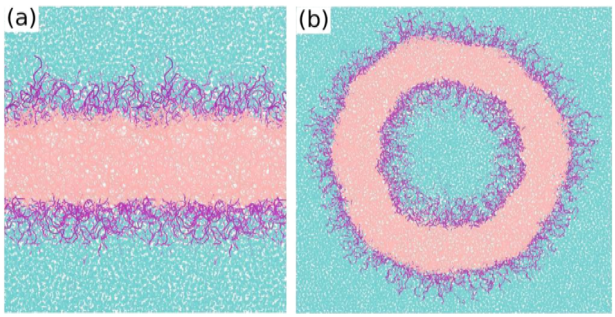

FIG. 2. Snapshots on equilibrium state for (a) neat bilayer and (b) neat polymersome. Components identified by color: PBD (pink), PEO (purple), water (cyan). Snapshots were generated using the VMD software.[48]

are compatible with a typical bilayer structure,[39] with the hydrophobic block (PBD) in the center, surrounded by the hydrophilic block (PEO) and water. The PEO MDPs are also similar in both systems, except for the asymmetry observed on the polymersome case. Here, the PEO density peak on the inner layer ($r \sim 8$ nm) presents a higher value compared to the PEO density peak on the outer layer ($r \sim 14$ nm).

The P_T and P_N profiles for the neat bilayer and polymersome are shown in Figs. 3(b)–3(d) respectively. For the neat bilayer, we observe that P_N is practically constant throughout the system and its average value is coincident to the external normal pressure (1 bar). This behavior is the expected one for planar systems in mechanical equilibrium.[57–59] The P_T profile is symmetric on the bilayer, where different contributions can be observed for each region. We identify a positive contribution in the PEO-water region, a negative one around the PEO-PBD interface and a positive one in the PBD region. These characteristics for the P_T profile were previously reported for PEO-PBD bilayers.[39] We have checked that the P_T values in the bulk water phase converge to the external tangential pressure (1 bar), as well as its mean value along the system.

For the neat polymersome, we observe some differences on the pressure profiles with respect to the bilayer case. The P_N profile is no longer constant; we identify a positive contribution in the region $r \lesssim 13.5$ nm with a maximum value at $r \sim 7.5$ nm, followed by a negative contribution that extends along the aqueous region, with a minimum at $r \sim 14$ nm. On the other hand, the P_T profile presents a similar shape to the one observed for the bilayer case but with differences in the pressure magnitudes accounting for the asymmetry around the mean radius ($r \sim 11$ nm). We observe a maximum P_T value at $r \sim 7$ nm (on the inner side of the polymersome) which is higher than the maximum observed at $r \sim 14.5$ nm (on the outer side). In the same way, the minimum P_T value observed at $r \sim 8$ nm (on the inner side) is lower than the minimum at $r \sim 13.5$ nm (on the outer side). In both cases, the P_N and P_T values in the bulk water phase converge to the external normal and tangential pressures (1 bar), as required for systems in mechanical equilibrium.

The elastic properties of the neat bilayer and polymersome were obtained by means of the Helfrich model (see Sec. II C 2). Within this framework, the elastic parameters of the membrane can be determined using the corresponding pressure profiles for each system (see calculation details on supplementary material).

For the neat bilayer, the resulting value for the spontaneous curvature was H_0 0.01 ± 0.02 nm^{-1} and for the elastic free energy was $f = 0.001 \pm 0.002$ nm^{-1} k_BT/nm^2. In this direction, we observe that H_0 and f are compatible to the condition of zero spontaneous curvature for symmetric bilayers.[53,56]

On the other hand, for the neat polymersome we calculated a spontaneous curvature of $H_0 = 0.69 \pm 0.03$ nm^{-1} and elastic free energy of $f = 44 \pm 3$ nm^{-1} k_BT/nm^2. Due to our convention of the curvature sign (see Sec. II C 2), the positive H_0 value can be interpreted as the tendency of the membrane to bulges locally towards the interior of the polymersome, favoring a lower membrane curvature and consequently a larger polymersome radius (see Refs. 60 and 61 for further details on the mechanism for spontaneous curvature on membranes). Moreover, we calculated from Eq. (5) the derivative of the elastic free energy with respect to the curvature (df/dH) evaluated on $H = 0$. For the neat polymersome, we obtained a value of $df/dH \simeq -38$ k_BT/nm^2, which implies that f decreases for greater H

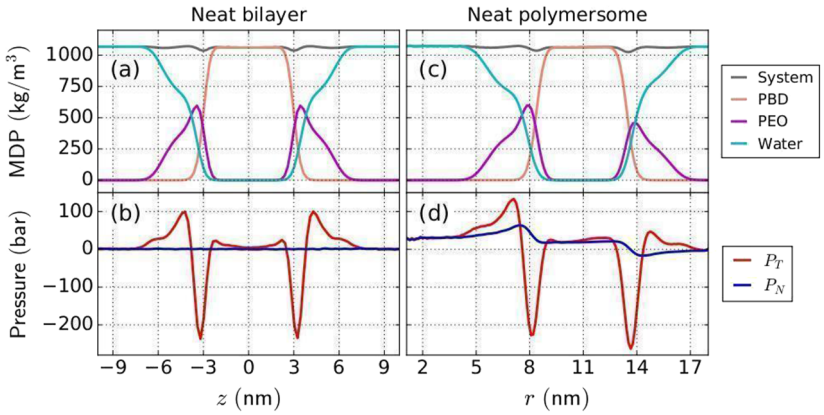

FIG. 3. MDPs of the total system, PBD, PEO and water components for (a) neat bilayer and (c) neat polymersome. P_T and P_N profiles for (b) neat bilayer and (d) neat polymersome.

values. Considering that $H = -1/R$ in our convention (R is the polymersome radius), increasing H leads to lower $|H|$, and hence larger R values. Therefore, a negative df/dH would indicate the tendency of the current neat polymersome towards larger radius, as previously suggested by the H_0 parameter.

B. Comparison of PLC-loaded systems

To evaluate the effect of the PLC loading on the systems structure, we have characterized the normalized membrane area expansion (α), the membrane thickness (d) and the hydrophobic volume per chain (V_{hc}) as function of the total number of PLC molecules ($N_{PLC} = N_{nPLC} + N_{pPLC}$) normalized by the number of copolymer chains in the system ($N_c = 200$ for bilayers and $N_c = 3141$ for polymersomes). For all PLC-loaded systems we have used N_{pPLC}/N_{nPLC} ratios corresponding to physiological pH considering Henderson-Hasselbalch equation (see Sec. II A). The corresponding results for α, d and V_{hc} are shown in Figs. 4(a)–4(c) respectively.

For bilayers we observe that the membrane area expands up to 15% [Fig. 4(a)] and the membrane thickness decreases [Fig. 4(b)] as PLC concentration increases. The same trend has been observed for bilayers loaded with pure pPLC,[39] suggesting that the structural characteristics of the PLC-loaded bilayers with the selected protonated/neutral ratio are dictated by the protonated species. This behavior can be explained by considering that the pPLC molecules, adsorbed at the PEO-PBD interfaces, induce a greater separation between the copolymer chains (area expansion); the latter ones are flexible enough to accommodate themselves within the structure, occupying the free spaces and leading to a membrane compression (d decrease). On the other hand, the effect of neutral species on the structure can be seen through the linear increase of V_{hc}. The green line in Fig. 4(c) represents the theoretical volume per chain occupied by nPLC molecules (estimated using the molar mass and the predicted PLC density[39]) as a function of the number of PLC molecules per chain in the system (where $N_{nPLC} = N_{PLC}/2.6$, obtained through the physiological pH ratio). As seen in Fig. 4(c), the V_{hc} values are well described by the green line, which indicates that the expansion of the hydrophobic core would correspond to the volume occupied by the nPLC molecules encapsulated into the membrane.

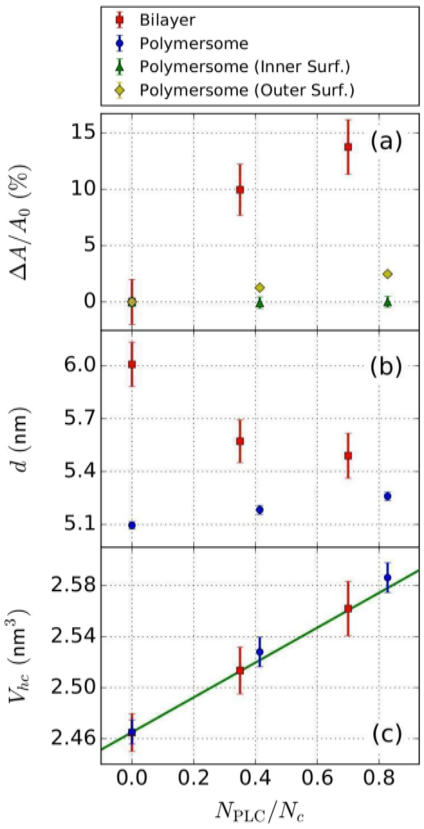

FIG. 4. Normalized area expansion (α), membrane thickness (d) and hydrophobic volume per chain (V_{hc}) as function of the number of PLC molecules per copolymer chain (N_{PLC}/N_c). In (a), one α value is determined for each bilayer (associated to the membrane area, A), while two α values were obtained for polymersomes (corresponding to the inner and outer membrane areas, A_i and A_o). In (c), the green line represents the theoretical volume per chain occupied by nPLC molecules as a function of the number of PLC molecules per chain.

For polymersomes, we observe that the inner membrane area remains constant while the outer membrane area slightly expands up to 2.5% as PLC concentration grows [Fig. 4(a)]. On the other hand, the membrane thickness also exhibits a slight increase in the same direction [see Fig. 4(b)]. This behavior, quite different from the one observed for bilayers, can be explained by the characteristics of the simulated polymersomes. As described above, the bilayers present a tangential expansion and normal compression with PLC loading.

In polymersomes, the tangential expansion of the membrane would lead to greater membrane areas and thus larger polymersomes. However, the simulation conditions (PBC and isotropic NPT ensemble) impose restrictions that constrain the box dimensions and maintain the system stability in the current configuration. Therefore, the size of the simulated polymersomes is essentially conserved (with a slight increase of the outer radius), frustrating the tangential expansion of the membrane. Because of this, the effect of the protonated species on the polymersome structure is canceled out. The slight increase of the membrane thickness with PLC concentration seems to be the result of the encapsulation of the neutral species within the membrane. The linear growth of V_{hc} following the green line [Fig. 4(c)] is consistent with this observation.

Snapshots of equilibrated PLC-loaded systems for the corresponding maximum PLC concentrations are depicted in Fig. 5. In both cases, we observe that the neutral PLC species (nPLC, green) are encapsulated within the hydrophobic core of the membrane (PBD, pink), while the protonated species (pPLC, red) are adsorbed on the membrane interface or distributed on the bulk water.

To describe the local distribution of the drug and their impact on the local pressure distribution across the systems, we analyze the MDPs of the nPLC and pPLC species and the $PT - PN$ profiles of the corresponding systems at different PLC concentrations. The resulting profiles are depicted in Fig. 6.

The local distributions of nPLC and pPLC on bilayers and polymersomes are shown in Figs. 6(a)–6(c) respectively. In both cases, the MPDs show that nPLC is localized within the PBD region and pPLC is distributed between the PEO-PBD interfaces and the water phase. For the polymersomes, the components are distributed in similar regions. The pPLC MDP presents density values at the outer

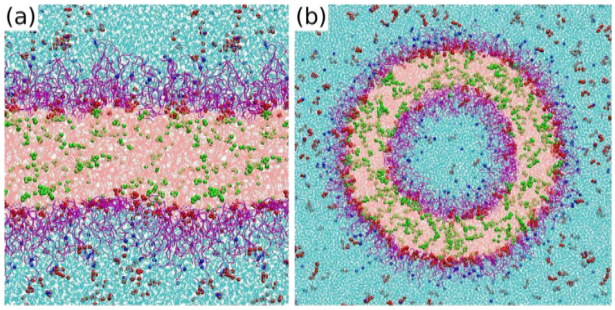

FIG. 5. Snapshots on equilibrium state for (a) PLC-loaded bilayer (N_{nPLC} = 54, N_{pPLC} = 86) and (b) PLC-loaded polymersome (N_{nPLC} = 1000, N_{pPLC} = 1600). Components identified by color: PBD (pink), PEO (purple), water (cyan), nPLC (green), pPLC (red), Cl^- (blue). Snapshots were generated using the VMD software.[48]

interface that are considerably higher than at the inner interface. On the contrary, the nPLC MDP is skewed towards the inner side. This may indicate that the neutral species would be accommodated in the structure to partially compensate for the imbalance observed on the pPLC distribution in favor of the outer side.

A better understanding of the mechanical behavior of the systems could be obtained by analyzing the $P_T - P_N$ profiles of bilayers and polymersomes as function of the PLC concentration [see Figs. 6(b)–6(d) respectively]. It is important to remark that the $P_T - P_N$ profiles provide a valuable tool for mechanical characterization since the elastic parameters of the membrane depend on their integral moments (see Sec. II C 2). For bilayers [Fig. 6(b)], we observe that the incorporation of PLC into the system leads to a narrowing of the $P_T - P_N$ profiles in z-direction [as consequence of the membrane thickness decrease, see Fig. 4(b)] without affecting significantly the local pressure distribution: the shape of the pressure profiles is essentially conserved, with some minor differences in the pressure values at the minima (located around the PEO-PBD interfaces). In this direction, the bilayer seems to be mechanically compliant to the PLC loading and relaxes its structure to allow the incorporation of the drug into the structure with low impact on its mechanical behavior.

For polymersomes [Fig. 6(d)], we observe that the PLC loading leads to significant changes in the $P_T - P_N$ profiles at the PEO-PBD interfaces ($r \sim 8$ nm and $r \sim 13.5$ nm), where $P_T - P_N$ values increase with the PLC concentration. We can also observe that the pressure increase for the minimum at $r \sim 13.5$ nm (outer PEO-PBD interface) is more pronounced than for the minimum at $r \sim 8$ nm (outer PEO-PBD interface). Analyzing the pPLC MDPs for polymersomes [see Fig. 6(b), full lines] we see that these pressure changes could be correlated to the amount of adsorbed PLC at the PEO-PBD interfaces: when the adsorbed pPLC density increases, the pressure value rises. This behavior could be explained by considering the effect of the protonated species on the structure. On bilayers, the adsorbed pPLC on the interfaces would be responsible for the tangential expansion of the membrane (as a consequence of the extra space occupied by these molecules), but this mechanism is frustrated in the polymersome, as already discussed in the analysis of structural parameters. In this direction, the increase of the pressure values at the interfaces could be a consequence of such frustration: the polymersome is not able to accommodate its structure to relax the local pressure generated by the pPLC molecules adsorbed at the interfaces, leading to a pressure increase proportional to the local pPLC concentration.

In order to obtain a deeper insight on the mechanical response of the systems upon PLC loading, we have analyzed the dependency of the elastic parameters of the membrane with PLC concentration. Since the interfaces seem to play a key role in the mechanical aspect, it would be interesting to connect these properties to the amount of adsorbed pPLC at the interfaces. To this end, we have characterized the difference of adsorbed pPLC molecules per unit area between interfaces ($\Delta\Gamma = \Gamma_{upp} - \Gamma_{low}$ for bilayers and $\Delta\Gamma = \Gamma_{out} - \Gamma_{inn}$ for polymersomes), the spontaneous curvature (H_0) and the elastic free energy per unit area (f) for all simulated systems. The results obtained for all simulated systems are shown in Table II.

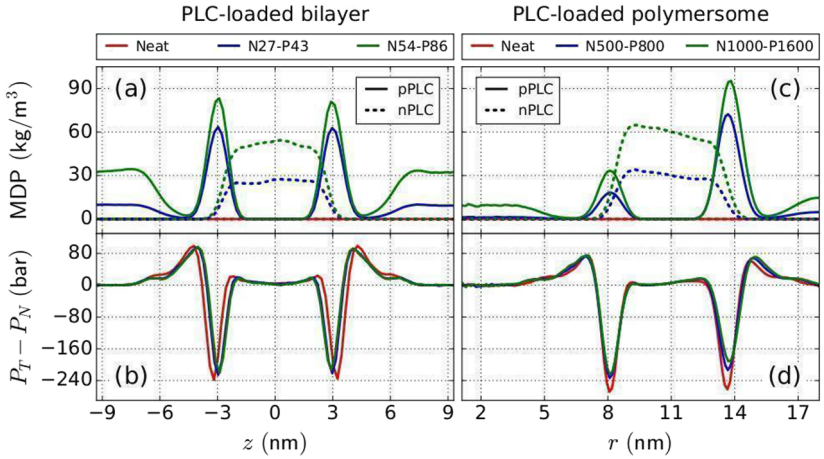

FIG. 6. MDPs of the nPLC and pPLC species at different PLC concentrations for (a) bilayers and (c) polymersomes. *PT − PN* profiles for the same PLC concentrations for (c) bilayers and (d) polymersomes. For all cases, we include the profiles of the corresponding neat systems as reference.

TABLE II. Difference of adsorbed pPLC molecules per unit area between interfaces ($\Delta\Gamma$), bending modulus (κ), Gaussian curvature modulus ($\bar{\kappa}$), spontaneous curvature (H_0), elastic free energy per unit area (f) and derivative of the elastic free energy respect to the curvature (df/dH) for all simulated systems. Notice that the parameter $\bar{\kappa}$ is not available for bilayers since the Gaussian curvature term vanishes at zero curvature. The quantity df/dH for bilayer was also calculated for bilayers, although not used in our analysis.

System[a]	$\Delta\Gamma$ (nm^{-2})	κ (k_BT)	$\bar{\kappa}$ (k_BT)	H_0 (nm^{-1})	f (k_BT/nm^2)	df/dH (k_BT/nm^3)
Neat (B)	0	12 ± 4	N/A	-0.006 ± 0.018	0.0008 ± 0.0018	0.3 ± 1.8
N27-P43 (B)	-0.01 ± 0.02	11 ± 3	N/A	0.03 ± 0.08	0.02 ± 0.04	-1 ± 7
N54-P86 (B)	-0.01 ± 0.03	10 ± 3	N/A	-0.002 ± 0.048	0.0001 ± 0.0012	0.07 ± 4.06
Neat (P)	0	39 ± 5	$-493/47$	0.69 ± 0.03	44 ± 3	-38 ± 2
N500-P800 (P)	0.13 ± 0.03	38 ± 5	$-356/60$	0.45 ± 0.03	19 ± 2	-22 ± 2
N1000-P1600 (P)	0.16 ± 0.03	38 ± 5	$-311/72$	0.33 ± 0.04	11 ± 2	-14 ± 2

[a](B) = Bilayer, (P) = Polymersome.

For bilayers, we observe that the number of adsorbed pPLC molecules per unit area in the upper and lower interfaces are statistically equal in all cases ($\Delta\Gamma \sim 0$), which reflects the symmetric nature of these systems. Similarly, to the neat case, the elastic parameters H_0 and f are also zero (within the statistical error) for PLC loaded bilayers.

For polymersomes we observe that $\Delta\Gamma$ increases with the PLC loading, which implies a greater amount of adsorbed pPLC on the outer interface compared to the inner one [see also pPLC MDP in Fig. 6(b)]. On the other hand, H_0 and f present positive but decreasing values as the PLC concentration increases. Due to the convention of the curvature sign (see Sec. II C 2), the positive H_0 values can be interpreted as the tendency of the membrane to curve towards the interior of the polymersome favoring lower curvature structures (thus larger polymersomes radii). As a consequence, the polymersome membrane becomes energetically more stable (lower f) and decreases its tendency to curve (lower H_0)) when $\Delta\Gamma$ increases.

To obtain a better understanding of the mechanical response of the systems in terms of curvature (H), we calculated the derivative of the elastic free energy with respect to the curvature [df/dH from Eq. (5)]. For the neat polymersome we have obtained $df/dH \simeq -38\ k_BT/nm^2$, which implies that f decreases for greater H values. Considering that $H = -1/R$ in our convention, where R is the polymersome radius (see Sec. II C 2), increasing H leads to lower $|H|$ and larger R values. When estimating df/dH for the PLC-loaded polymersomes, we have obtained the approximated values $-22\ k_BT/nm^2$ and $-14\ k_B/nm^2$ for N500-P800 and N1000-P1600 polymersomes respectively. Compared to the neat case, we see that the df/dH values are also negative but decrease in absolute value, indicating that the curvature change required to minimize the elastic energy of the membrane would be lower for greater PLC concentrations. This means that the polymersome configuration becomes more stable when the PLC concentration grows, which is consistent with the previous observation of lower f for higher PLC levels. Besides, pPLC partitions between water and hydrophilic regions and considering that the hydrophilic crown of the inner shell is more compact than the outer one, the inner shell show less capacity to host pPLC than the outer shell.

Our results suggest that the initial (neat) polymersome is highly curved on the current configuration, showing a tendency to form lower curvature polymersomes (greater radius); this tendency to curve decreases as $\Delta\Gamma$ increases with the PLC loading. This behavior could be explained in terms of the local pressure distribution: the initial polymersome presents a lateral pressure imbalance that pushes the membrane to greater lateral expansions on the inner side, generating the observed tendency to lower curvatures. When PLC is incorporated into the system, the excess of adsorbed pPLC on the outer interface provides extra pressure on the outer side that reduces the initial pressure imbalance between interfaces, decreasing the tendency of the membrane to curve and stabilizing the system in the current configuration. The hypothesis of the lateral pressure increase on the outer interface is consistent with the pressure changes observed on the $P_T - P_N$ profiles at the interfaces [see Fig. 6(d)].

V. CONCLUSIONS AND PERSPECTIVES

In this work, we have implemented a computational method to determine structural and mechanical properties of planar and spherical bilayers using Molecular Dynamics simulations. The method includes the calculation of key structural membrane parameters from mass density profiles, and determination of curvature elastic parameters from pressure profiles.

The methodology was applied to characterize PEO-PBD bilayers and polymersomes loaded with a combination of neutral and protonated Prilocaine. The studies were carried out using MD simulations performed within the CG MARTINI model using different PLC concentrations at physiological pH levels (pPLC/nPLC $\simeq$ 1.6). The obtained results show that in bilayers and vesicles systems, the neutral species are encapsulated within the hydrophobic core, while the protonated ones are adsorbed on the PEO-PBD interfaces or distributed in the aqueous phase as have already seen in previous work. In particular, for bilayers, we observe that the structural behavior of the systems is guided by the protonated species: lateral membrane expansion (area increase) and normal membrane compression (thickness decrease) as PLC concentration increases. In all cases, the bilayer shows a symmetric distribution around its midplane. As a consequence of this symmetry, the difference of pPLC adsorbed on both interfaces ($\Delta\Gamma$), the spontaneous curvature (H_0) and the elastic free energy (f) are zero within the statistical error.

For polymersomes we observe that the structural behavior is driven by the neutral species: a slight expansion of the membrane in the normal direction is only seen. In this case, due to the limitations imposed by the simulation conditions, the lateral expansion of the membrane induced by the protonated species is frustrated

in the polymersome, leading to important consequences at the mechanical level. We observe that $\Delta\Gamma$ increases but H_0 and f both decrease with PLC concentration. A possible interpretation for this behavior is that the initial (neat) polymersome presents a lateral pressure imbalance that promotes a greater membrane expansion on the inner interface, causing a tendency to reduce its curvature and to increase its radius. Then, the greater adsorption of pPLC on the outer interface provides an extra lateral pressure on this region, reducing the initial lateral pressure imbalance and thus decreasing the tendency to curve and the elastic energy accumulated in the membrane. In this direction, the presence of the drug seems to stabilize the membrane in this particular polymersome configuration. At this point, there are two factors that could play a key role, the size of the polymersome that determines the current membrane curvature, and the number of chains in both layers. For each polymersome at a given radius, it could be possible to find an optimal relationship between the number of inner/outer chains that balance the distribution of lateral pressures, in such a way that the tendency to curve and the elastic energy are minimal. In this direction, the analysis of the elastic parameters could be used to explore and determine optimal inner/outer chain ratios for the most stable size vesicle.

As a general conclusion, we can state that both models (bilayers and polymersomes) are useful for the study of drug encapsulation in polymer membranes. Both systems have complementary features, being the bilayer model less computer resource demanding and more suitable for the structural characterization of the membrane (area per chain and membrane thickness), and the polymersome model for its mechanical characterization (spontaneous curvature and elastic free energy). In particular, in the latter model, although the structural response is restricted by the simulation conditions, the elastic parameters could be the driving factors in the search of the optimal configuration.

Due to the computational cost to study entire polymerssome, bilayers are broadly used as models. Here we provided a comparison between them and important features were found. It is important to point out that here that we investigated a particular stable polymersome. Stable polymersome are not unique. Experimentally, it can have different radii and consequently curvatures.

As perspectives, we believe that the methodology presented in this work may be a valuable tool in general problems with planar and spherical symmetries. In particular, as we showed here, it could be useful to study systems on the design and characterization of mechanically stable polymersomes for drug delivery applications. Bilayer simulations could be used to explore different materials and formulations to determine polymer membranes with desired properties. Polymersomes of selected materials could be simulated, using different sizes and/or different inner/outer chain ratios, to obtain the most stable prospects (e.g., the polymersome with the lowest elastic free energy). Finally, the effect of the drug loading on the mechanical and elastic behavior of the most promising candidates can be studied to determine their stability as drug carriers.

SUPPLEMENTARY MATERIAL

The supplementary material contains the following information:

- Calculation of adsorbed pPLC molecules per unit area.
- Calculation of elastic parameters of bilayers and polymersomes.
- Calculation of bending modulus of bilayers and polymersomes.

ACKNOWLEDGMENTS

This work was developed with financial support from Universidad de Buenos Aires (Grant No. UBA- CYT 20020170100456BA), CONICET (Grant No. PIP 11220200100467CO), and ANPCyT (Grant Nos. PICT2019-2108 and PICT-2019-1045). Generous allocation in Center of High Performance Computing (CHPC) of the University of Utah partially funded by NIH Research Instrumentation Award Grant No. S10OD021644 is gratefully acknowledged.

AUTHOR DECLARATIONS

Conflict of Interest

The authors have no conflicts to disclose.

Author Contributions

Damián A. Grillo: Conceptualization (equal); Data curation (equal); Formal analysis (equal); Investigation (equal); Methodology (equal); Software (equal); Validation (equal); Writing – original draft (equal). **Juan M. R. Albano**: Conceptualization (equal); Data curation (equal); Investigation (equal); Methodology (equal); Software (equal). **Rufino E. Valladares T.**: Conceptualization (equal); Investigation (equal); Writing – original draft (equal). **Esteban E. Mocskos**: Conceptualization (equal); Methodology (equal); Validation (equal). **Julio C. Facelli**: Conceptualization (equal); Funding acquisition (equal); Supervision (equal); Writing – original draft (equal). **Mónica Pickholz**: Conceptualization (equal); Data curation (equal); Formal analysis (equal); Funding acquisition (equal); Investigation (equal); Methodology (equal); Supervision (equal); Writing – original draft (equal). **Marta B. Ferraro**: Conceptualization (equal); Data curation (equal); Funding acquisition (equal); Investigation (equal); Methodology (equal); Project administration (equal); Supervision (equal); Writing – original draft (equal).

DATA AVAILABILITY

The data that support the findings of this study are available from the corresponding author upon reasonable request.

REFERENCES

[1] K. R. Gajbhiye, R. Salve, M. Narwade, A. Sheikh, P. Kesharwani, and V. Gajbhiye, Mol. Cancer **22**, 160 (2023).
[2] Y. Zhao, T. Irie, J. Sakai, H. Mabuchi, S. Biswas, T. Sekine, S. Das, T. Ben, and Y. Negishi, ACS Appl. Nano Mater. **6**, 19210 (2023).
[3] M. A. Waqar, M. Zamán, H. Hameed, M. Jamshaid, A. Irfan, G. A. Shazly, A. C. Paiva Santos, and Y. A. Bin Jardan, ACS Omega **8**, 38191 (2023).
[4] L. Huang, Z. Sun, Q. Shen, Z. Huang, S. Wang, N. Yang, G. Li, Q. Wu, W. Wang, L. Li, and C. Yu, Chin. Chem. Lett. **33**, 4146 (2022).
[5] R. Rodriguez-Garcia, M. Mell, I. Lopez-Montero, J. Netzel, T. Hellweg, and F. Monroy, Soft Matter **7**, 1532 (2011).

[6]H.-Y. Chang, Y.-J. Sheng, and H.-K. Tsao, Soft Matter **10**, 6373 (2014).
[7]K. Jaskiewicz, M. Makowski, M. Kappl, K. Landfester, and A. Kroeger, Langmuir **28**, 12629 (2012).
[8]N. Machado, B. M. H. Bruininks, P. Singh, L. dos Santos, C. Dal Pizzol, G. de C. Dieamant, O. Kruger, A. A. Martin, S. J. Marrink, P. C. T. Souza, and P. P. Favero, Nanoscale **14**(2), 506 (2022).
[9]Y. Song, J. H. Lee, I. Jung, B. Seo, and H. Hwang, J. Phys. Chem. B **124**, 5919 (2020).
[10]L. Razavi, H. Raissi, and F. Farzad, Sci. Rep. **13**, 2665 (2023).
[11]H. Hashemzadeh, H. Javadi, and M. H. Darvishi, Sci. Rep. **10**, 1837 (2020).
[12]Y.-L. Lin, H.-Y. Chang, Y.-J. Sheng, and H.-K. Tsao, Soft Matter **9**, 4802 (2013).
[13]V. Kozlovskaya, M. Ducharme, M. Dolmat, J. M. Omweri, V. Tekin, S. E. Lapi, and E. Kharlampieva, Biomacromolecules **24**, 1784 (2023).
[14]D. Rahmani, N. A. Torbat, and S. Boddohi, Eur. Polym. J. **191**, 112032 (2023).
[15]B. Kiani-Dehkordi, A. Vatanara, M. Amini, M. Hamidi, M. Dibaei, P. Norouzi, S. Rezaei, A. Khoshnazar, and M. R. Rouini, Mater. Today Chem. **30**, 101504 (2023).
[16]R. El Yousfi, M. Brahmi, M. Dalli, N. Achalhi, O. Azougagh, A. Tahani, R. Touzani, and A. El Idrissi, Polymers **15**, 1835 (2023).
[17]B. M. Discher, Y.-Y. Won, D. S. Ege, J. C.-M. Lee, F. S. Bates, D. E. Discher, and D. A. Hammer, Science **284**, 1143 (1999).
[18]J. F. Le Meins, O. Sandre, and S. Lecommandoux, Eur. Phys. J. E **34**, 14 (2011).
[19]J. Du and R. K. O'Reilly, Soft Matter **5**, 3544 (2009).
[20]A. Blanazs, S. P. Armes, and A. J. Ryan, Macromol. Rapid Commun. **30**, 267 (2009).
[21]R. P. Brinkhuis, F. P. J. T. Rutjes, and J. C. M. van Hest, Polym. Chem. **2**, 1449 (2011).
[22]J. Lefley, C. Waldron, and C. R. Becer, Polym. Chem. **11**, 7124 (2020).
[23]C. G. Palivan, R. Goers, A. Najer, X. Zhang, A. Car, and W. Meier, Chem. Soc. Rev. **45**, 377 (2016).
[24]L. Messager, J. Gaitzsch, L. Chierico, and G. Battaglia, Curr. Opin. Pharmacol. **18**, 104 (2014).
[25]T. Anajafi and S. Mallik, Ther. Delivery **6**, 521 (2015).
[26]D. E. Discher and F. Ahmed, Annu. Rev. Biomed. Eng. **8**, 323 (2006).
[27]M. Hasannia, A. Aliabadi, K. Abnous, S. M. Taghdisi, M. Ramezani, and M. Alibolandi, J. Controlled Release **341**, 95 (2022).
[28]S. Iqbal, M. Blenner, A. Alexander-Bryant, and J. Larsen, Biomacromolecules **21**, 1327 (2020).
[29]P. Tanner, P. Baumann, R. Enea, O. Onaca, C. Palivan, and W. Meier, Acc. Chem. Res. **44**, 1039 (2011).
[30]W. Helfrich, Z. Naturforsch. C **28**, 693 (1973).
[31]W. Helfrich, J. Phys. France **47**, 321 (1986).
[32]T. Nakamura and W. Shinoda, J. Chem. Phys. **138**, 124903 (2013).
[33]S. J. Marrink and A. E. Mark, J. Am. Chem. Soc. **125**, 15233 (2003).
[34]L. Gao, J. Shillcock, and R. Lipowsky, J. Chem. Phys. **126**, 015101 (2007).
[35]J. C. Shillcock and R. Lipowsky, J. Chem. Phys. **117**, 5048 (2002).
[36]S. J. Marrink, H. J. Risselada, S. Yefimov, D. P. Tieleman, and A. H. de Vries, J. Phys. Chem. B **111**, 7812 (2007).
[37]D. H. de Jong, G. Singh, W. F. D. Bennett, C. Arnarez, T. A. Wassenaar, L. V. Schäfer, X. Periole, D. P. Tieleman, and S. J. Marrink, J. Chem. Theory Comput. **9**, 687 (2013).
[38]M. Pickholz and G. Giupponi, J. Phys. Chem. B **114**, 7009 (2010).
[39]D. A. Grillo, J. M. R. Albano, E. E. Mocskos, J. C. Facelli, M. Pickholz, and M. B. Ferraro, J. Chem. Phys. **146**, 244904 (2017).
[40]S. O. Yesylevskyy, L. V. Schäfer, D. Sengupta, and S. J. Marrink, PLoS Comput. Biol. **6**, e1000810 (2010).
[41]L. Martínez, R. Andrade, E. G. Birgin, and J. M. Martínez, J. Comput. Chem. **30**, 2157 (2009).
[42]L. Bai and D. Breen, J. Graphics Tools **13**, 53 (2008).
[43]D. J. Evans and B. L. Holian, J. Chem. Phys. **83**, 4069 (1985).
[44]M. Parrinello and A. Rahman, J. Appl. Phys. **52**, 7182 (1981).
[45]B. Hess, H. Bekker, H. J. C. Berendsen, and J. G. E. M. Fraaije, J. Comput. Chem. **18**, 1463 (1997).
[46]J. Walton, D. Tildesley, J. Rowlinson, and J. Henderson, Mol. Phys. **48**, 1357 (1983).
[47]O. H. S. Ollila, H. J. Risselada, M. Louhivuori, E. Lindahl, I. Vattulainen, and S. J. Marrink, Phys. Rev. Lett. **102**, 078101 (2009).
[48]R. Goetz and R. Lipowsky, J. Chem. Phys. **108**, 7397 (1998).
[49]E. Lindahl and O. Edholm, J. Chem. Phys. **113**, 3882 (2000).
[50]J. Gullingsrud and K. Schulten, Biophys. J. **86**, 3496 (2004).
[51]J. Sonne, F. Y. Hansen, and G. H. Peters, J. Chem. Phys. **122**, 124903 (2005).
[52]T. Nakamura, W. Shinoda, and T. Ikeshoji, J. Chem. Phys. **135**, 094106 (2011).
[53]D. Marsh, Chem. Phys. Lipids **144**, 146 (2006).
[54]I. Szleifer, D. Kramer, A. BenShaul, W. M. Gelbart, and S. A. Safran, J. Chem. Phys. **92**, 6800 (1990).
[55]B. Rózycki and R. Lipowsky, J. Chem. Phys. **142**, 054101 (2015).
[56]X. Wang and M. Deserno, J. Chem. Phys. **143**, 164109 (2015).
[57]J. S. Rowlinson and B. Widom, *Molecular Theory of Capillarity* (Clarendon Press, Oxford, 1982).
[58]F. Varnik, J. Baschnagel, and K. Binder, J. Chem. Phys. **113**, 4444 (2000).
[59]M. Orsi and J. W. Essex, Faraday Discuss. **161**, 249 (2013).
[60]R. Lipowsky, Faraday Discuss. **161**, 305 (2013).
[61]R. Lipowsky, Adv. Colloid Interface Sci. **208**, 14 (2014), part of Special Issue in Honour of Wolfgang Helfrich.